Eur J Nucl Med Mol Imaging (2010) 37:1291–1299
DOI 10.1007/s00259-010-1412-6

ORIGINAL ARTICLE

Imaging of proliferation with ^{18}F-FLT PET/CT versus ^{18}F-FDG PET/CT in non-small-cell lung cancer

Wenfeng Yang · Yongming Zhang · Zheng Fu · Jinming Yu · Xiaorong Sun · Dianbin Mu · Anqin Han

Received: 14 November 2009 / Accepted: 5 February 2010 / Published online: 23 March 2010

Abstract
Purpose To compare the diagnostic efficacies of ^{18}F-FLT and ^{18}F-FDG PET/CT in non-small-cell lung cancer (NSCLC), focusing on the correlation between FLT and FDG tumour uptake and tumour cell proliferation as indicated by the cyclin D1 labelling index.
Methods A total of 31 patients with NSCLC underwent FLT and FDG PET/CT scanning followed by surgery. PET/CT images were compared with the pathology. Tumour cell proliferation was assessed by cyclin D1 immunohistochemistry.
Results The sensitivities of FLT and FDG PET/CT for the primary lesion were 74% and 94%, respectively (p=0.031). For N staging, 77% patients were correctly staged, 6% overstaged, 16% understaged by FLT, while the values for FDG were 77%, 16% and 6%, respectively. The sensitivity, specificity, accuracy, and positive predictive value with FLT for lymph nodes were 65%, 98%, 93% and 89%, respectively, and 85%, 84%, 84% and 52% with FDG (p<0.01).Tumour SUV of FLT was significantly correlated with the cyclin D1 labelling index (r=0.644; p<0.01), but the SUV of FDG was not significantly correlated (r=0.293; p>0.05).
Conclusion In terms of N staging, FLT PET/CT resulted in understaging of more patients but overstaging of fewer patients, and for regional lymph nodes showed better specificity, accuracy and positive predictive value than FDG PET/CT in NSCLC. Tumour FLT uptake was correlated with tumour cell proliferation as indicated by the cyclin D1 labelling index, suggesting that further studies are needed to evaluate the use of FLT PET/CT for the assessment of therapy response to anticancer drugs.

Keywords Non-small-cell lung cancer · ^{18}F-FLT PET/CT · ^{18}F-FDG PET/CT · Cyclin D1

W. Yang · Y. Zhang
Department of Thoracic Surgery,
Shandong Cancer Hospital and Institute,
Jinan 250117 Shandong Province, People's Republic of China

Z. Fu · X. Sun · A. Han
Department of Nuclear Medicine,
Shandong Cancer Hospital and Institute,
Jinan 250117 Shandong Province, People's Republic of China

J. Yu (✉)
Department of Radiation Oncology,
Shandong Cancer Hospital and Institute,
Jiyan Road 440,
Jinan 250117 Shandong Province, People's Republic of China
e-mail: yujinmingsd@yahoo.com.cn

D. Mu
Department of Pathology,
Shandong Cancer Hospital and Institute,
Jinan 250117 Shandong Province, People's Republic of China

Introduction

Positron emission tomography (PET) with ^{18}F-fluorodeoxyglucose (FDG) and PET/CT is now used to diagnose, stage, and monitor the effects of treatment in lung cancer patients [1]. However, FDG is not a tumour-specific tracer, and false-positive findings can occur in inflammatory lesions [2, 3]. The thymidine analogue ^{18}F-labelled 3′-deoxy-3′-fluorothymidine (^{18}F-FLT) as a stable tumour cell proliferation imaging agent has been widely used in humans [4]. Imaging of cellular proliferation provides an alternative noninvasive approach to the diagnosis and staging of lung cancer, and more important is the possibility that such imaging could be used to predict the treatment

response in individual patients soon after the initiation of antitumour therapy.

Uncontrolled cell proliferation is the primary hallmark of cancer. The rate of cell division is an important prognostic characteristic of malignancies, and some important anticancer treatments are aimed specifically at inhibiting tumour cell growth. Some studies have demonstrated that the proliferative activity as determined by the expression levels of Ki-67 [5] and cyclin D1 [6–9] are important prognostic factors in non-small-cell lung cancer (NSCLC), and have found significant correlations between the standardized uptake value (SUV) of FLT and Ki-67 proliferation scores [10, 11]. But few studies have investigated the relationship between the imaging of cell proliferation and the cyclin D1 expression.

Cyclin D1 is known to regulate the G_1 to S phase transition during the cell cycle. Deregulated pathways governing the cell cycle have been recognized as a primary factor in the development of malignancy. Cyclin D1 overexpression is rather a pivotal element in the process of malignant transformation in lung cancer, and new therapies in lung cancer targeting the tumour cell proliferation cycle have emerged. In this study, we compared FLT and FDG PET/CT imaging in the diagnosis and staging of NSCLC. We focused on the correlation between FLT and FDG tumour uptake and tumour cell proliferation as indicated by the cyclin D1 labelling index.

Methods

Patients

The patients with NSCLC enrolled in this prospective study all underwent conventional lung cancer staging on the basis of clinical information, and both FLT and FDG PET/CT studies. The exclusion criteria were allergy to iodine contrast agent and hyperglycaemia of more than 9 mmol/l on the day the PET/CT scan was performed. Patients with other extrathoracic metastasis and those who had received prior chemotherapy or radiotherapy were also excluded. Thus, 31 patients (22 men and 9 women; mean age 59 years, range 38 to 84 years) were included in the study. ^{18}F-FLT and ^{18}F-FDG PET/CT examinations were performed on consecutive days during the 2 weeks before surgery. The pathological results served as the reference standards. Tumour stages were classified according to the IASLC Lung Cancer Staging Project [12]. This study protocol was approved by the institutional review board of our hospital, and informed consent was obtained from each patient.

PET/CT scanning

Both ^{18}F-FLT and ^{18}F-FDG were synthesized in our imaging centre with a radiochemical yield of >10% and a radiochemical purity of >95%. All patients fasted for at least 6 h before examination. They then received an intravenous injection of 300–400 MBq radioactive tracer, and rested for approximately 60 min before scanning. Scanning was performed with an integrated in-line PET/CT system (Discovery LS; GE Healthcare). An unenhanced CT scan was performed first, from the head to the thigh, with the following settings: 140 kV, 80 mAs, tube rotation time 0.5 s per rotation, pitch 0.75, and section thickness 4.25 mm, which matched the PET section thickness. A PET emission scan was performed that covered the identical transverse field of view immediately after the CT scan. The acquisition time for the PET scan was 4 min per table position. Patients were in normal shallow respiration during image acquisition. PET datasets were reconstructed iteratively using the CT data for attenuation correction, and coregistered images were displayed on a workstation (Xeleris; GE Healthcare).

Two experienced nuclear medicine physicians, unaware of surgical or pathologic findings and any clinical information except the patients with NSCLC, prospectively interpreted PET/CT images, only one final decision was made by these two physicians. Tumour lesions were identified as areas of focally increased uptake exceeding that of the surrounding normal tissue. For primary tumours visualized on PET, a region of interest (ROI) was placed over the entire FLT- or FDG-avid lesion on all transverse planes in which the tumour appeared. The maximum SUV (SUVmax) was calculated using the formula $SUV = c_{dc}/(d_i/w)$, where c_{dc} is the decay-corrected tracer tissue concentration (in becquerels per gram), d_i is the injected dose (in becquerels), and w is the patient's body weight (in grams) [13]. For lesions not visible on both or either of the two PET scans, an ROI was drawn on the respective scans in the area corresponding to the area of abnormality on the CT image. Lesions were considered positive if a definite, localized area of higher ^{18}F-FDG or ^{18}F-FLT uptake than in the surrounding normal tissue was present, excluding physiological uptake.

Immunohistochemical staining with cyclin D1

The standard streptavidin-biotin immunoperoxidase method (Dako universal kit; Dako Corporation, Carpinteria, CA) was used on 4-mm sections of formalin-fixed, paraffin-embedded tissue after deparaffinization and antigen retrieval. The monoclonal murine cyclin D1 antibody (DCS-6; DakoCytomation, Denmark; 1:40 dilution) was used.

Diaminobenzidine was used as the final chromogen and haematoxylin as the nuclear counterstain. Positive controls were included in each experiment and consisted of tissue that had been stained previously specifically for the target antigen after exposure to primary antibody. Negative controls for each tissue section were performed using normal mouse serum (Dako) in place of the primary antibody; no significant staining was observed in the negative controls. The cyclin D1 labelling index reflects cell proliferation and was defined as the percentage of nuclei stained per total number of nuclei in the sample. The percentage score was determined by counting the cyclin D1-positive nuclei per 1,000 tumour cells in the region of the tumour with the greatest density of staining, which in most instances corresponds to areas with the highest mitotic activity. The pathologist was unaware of the results from the PET/CT imaging.

Statistical analysis

Statistical analyses were performed using the SPSS statistical software program (version 12.0 for Windows). The results of the imaging of fused FLT and FDG PET/CT were compared with a reference standard provided by pathological examination. Sensitivity, specificity, accuracy, positive predictive value and negative predictive value of FLT and FDG PET/CT for the detection of the lesion were calculated, and statistical significance was determined with the McNemar test. The correlation between FLT and FDG uptakes and cyclin D1 labelling index was assessed using linear regression analysis. The significance of differences between the mean SUVmax of ^{18}F-FLT and ^{18}F-FDG in the primary lesion was determined using the *t* test, and the significance of differences among the pathological subtypes and levels of differentiation were determined using one-way ANOVA. Statistical significance was assumed for *p* values less than 0.05.

Results

Pathological findings

Pathological analysis revealed adenocarcinoma in 13 patients, squamous cell carcinoma in 11, adenosquamous carcinoma (showing components of both squamous cell carcinoma and adenocarcinoma, with each comprising at least 10% of the whole tumour) in 3, bronchoalveolar carcinoma in 2, and large-cell neuroendocrine cancer in 2. Well-differentiated carcinoma was seen in 10 patients, moderately differentiated carcinoma in 13, and poorly differentiated carcinoma in 8.

A total of 356 lymph nodes in the NSCLC patients were sampled for pathological analysis. Of these, 17% (60 of 356) from 18 patients proved to be positive for malignancy, and of these 60, 43 (72%) were hilar and interlobar nodes (N1 nodal station). The pathological analysis in the 31 patients revealed tumour stages of IA in 4 patients, IB in 4, IIA in 10, IIB in 4, and IIIA in 9 (Tables 1 and 2). The pathological examination showed that the lymph nodes false-positive on imaging with FLT showed reactive hyperplasia and inflammation.

FLT and FDG PET/CT findings

For depiction of the primary lesion, the sensitivity of FLT PET/CT was 74% (23 of 31), compared with 94% (29 of 31) for FDG PET/CT (p=0.031, McNemar test). The sensitivity, specificity, accuracy, positive predictive value, and negative predictive value of FLT PET/CT for lymph nodes were 65%, 98%, 93%, 89% and 94%, respectively; compared with 85%, 84%, 84%, 52% and 96% for FDG PET/CT (p=0.0001, 0.0001, 0.0001, 0.001, 0.086, respectively, McNemar test). For N staging, 77% of patients were correctly staged, 6% of patients overstaged (false-positive), and 16% understaged (false-negative) with FLT PET/CT, while for FDG PET/CT these values were 77%, 16%, and 6%, respectively (Fig. 1, Tables 2 and 3). The mean ^{18}F-FLT SUVmax (4.2±3.3) in primary tumours was significantly lower than the mean ^{18}F-FDG SUVmax (7.7±4.9; t=3.24, p=0.002, t test), but linear regression analysis indicated that there was a significant correlation between them (r=0.53, p=0.003). The mean SUVmax values of ^{18}F-FLT and ^{18}F-FDG in the primary lesions were significantly different among the pathological stages, with the higher SUVmax in patients with a more advanced stage, but there was no significant difference among the pathological subtypes or among the levels of differentiation (Table 4).

Cyclin D1 immunohistochemistry

Cycling D1 immunohistochemical staining was evaluated for 31 primary lesions (one cyclin D1-stained tissue sample from each patient). The cyclin D1 index averaged 29.6±24.8%, ranging from 0 to 75% (Table 1).

Correlation of FLT and FDG uptake with cyclin D1

Only primary lesions were included in this analysis because nodal involvement by malignancy occurred in several patients in a small area of the lymph node, and cyclin D1 staining was probably not performed on the most representative section of the lymph nodes since serial sectioning was not routinely carried out.

Table 1 Clinical data and PET/CT findings in the 31 patients

Patient no.	Age (years)	Sex	Histology	Pathological stage (pT N M0)	FLT PET		FDG PET		Cyclin D1 labelling index (%)
					Primary SUV max	N stage	Primary SUV max	N stage	
1	57	M	Squamous cell carcinoma	pT3N1	6.1	N2	8.4	N2	39.0
2	83	M	Squamous cell carcinoma	pT2N1	7.2	N1	9.1	N1	19.0
3	43	M	Adenosquamous carcinoma	pT1N1	2.4	N1	6.9	N1	18.0
4	73	F	Adenocarcinoma	pT3N0	4.0	N0	17.6	N1	14.0
5	60	M	Adenocarcinoma	pT1N2	1.2	N0	2.6	N0	4.2
6	67	M	Large cell neuroendocrine cancer	pT2N0	4.8	N0	8.2	N0	37.0
7	38	F	Squamous cell carcinoma	pT1N0	0.7	N0	2.0	N0	0
8	61	F	Adenocarcinoma	pT2N0	1.0	N0	4.1	N0	1.4
9	56	M	Squamous cell carcinoma	pT2 N2	10.7	N2	8.9	N2	75.0
10	84	M	Squamous cell carcinoma	pT1 N1	1.1	N0	3.4	N1	1.9
11	59	M	Adenocarcinoma	pT1 N2	8.1	N1	10.1	N2	30.0
12	47	F	Bronchoalveolar carcinoma	pT2N0	1.3	N0	2.8	N0	4.8
13	41	M	Adenocarcinoma	pT3N0	6.6	N1	17.5	N1	52.0
14	73	M	Adenocarcinoma	pT1N1	1.4	N0	7.1	N0	4.3
15	71	M	Adenosquamous carcinoma	pT2N1	4.6	N1	6.2	N1	9.0
16	49	F	Bronchoalveolar carcinoma	pT1N1	1.8	N0	2.8	N1	44.0
17	53	M	Adenocarcinoma	pT3N2	9.4	N2	9.6	N2	35.0
18	43	M	Adenocarcinoma	pT3N0	2.3	N0	2.8	N0	71.0
19	52	F	Adenosquamous carcinoma	pT2N0	3.4	N0	5.2	N0	30.0
20	77	M	Adenocarcinoma	pT2N0	3.8	N0	3.5	N0	27.0
21	39	M	Large cell neuroendocrine cancer	pT1 N0	0.8	N0	6.7	N0	2.6
22	60	F	Adenocarcinoma	pT2 N2	3.0	N2	10.0	N2	36.0
23	56	M	Adenocarcinoma	pT2N0	5.1	N0	18.3	N2	58.0
24	80	M	Adenocarcinoma	pT1 N0	0.9	N0	1.7	N0	4.2
25	67	F	Squamous cell carcinoma	pT2 N1	5.3	N1	7.1	N1	68.0
26	46	M	Squamous cell carcinoma	pT1 N0	0.5	N0	3.0	N0	2.3
27	64	M	Squamous cell carcinoma	pT3 N1	7.0	N1	6.7	N1	49.0
28	56	F	Adenocarcinoma	pT1 N1	3.0	N1	4.9	N1	66.0
29	48	M	Squamous cell carcinoma	pT3 N1	8.3	N1	8.9	N1	44.0
30	73	M	Squamous cell carcinoma	pT2N1	2.5	N1	17.3	N2	3.4
31	64	M	Squamous cell carcinoma	pT3 N2	13.1	N2	14.5	N2	69.0

In 31 pulmonary lesions, linear regression analysis indicated that tumour FLT SUVmax values were significantly correlated with cyclin D1 index (r=0.644, p=0.0001). However, the FDG SUV max was not significantly correlated (r=0.293, p=0.110; Fig. 2).

Discussion

Detection of FLT and FDG PET/CT for the NSCLC patients

In the present study, the mean FLT SUVmax (4.2±3.3) in primary tumours was significantly lower than the mean FDG SUVmax (7.7±4.9), which is consistent with the findings of recent studies [14]. Buck et al. reported that ^{18}F-FLT uptake is only 50% of ^{18}F-FDG uptake in positive nodal metastases of NSCLC [10, 14]. This is mainly due to the imaging characteristics of the two tracers. ^{18}F-FLT uptake is related to cellular proliferation, whereas ^{18}F-FDG uptake is related to increased glucose metabolism. Because most cancer cells are metabolically active but fewer cells are proliferating, a higher net uptake of ^{18}F-FDG than of ^{18}F-FLT in the tumour can be expected. Furthermore, the study showed there is a significant correlation between the mean SUVmax of ^{18}F-FLT and that of ^{18}F-FDG. The mean SUVmax values of ^{18}F-FLT and ^{18}F-FDG in the primary lesions were higher in those with more advanced patholog-

Table 2 Results of FLT and FDG PET/CT imaging in differentiating between N0, N1, and N2 status in the 31 NSCLC patients

PET/CT	Pathological N stage			
	N0 (*n*=13)	N1 (*n*=12)	N2 (*n*=6)	Total (*n*=31)
FLT				
N0	12	3	1	16
N1	1	8	1	10
N2	0	1	4	5
FDG				
N0	10	1	1	12
N1	2	9	0	11
N2	1	2	5	8

ical stages, but the lower level of FLT uptake probably decreased the detection limit, making it more difficult to visualize the lesion, and increased the false-negative rate.

This study showed that 74% of all histologically verified primary tumours were correctly identified by FLT PET/CT compared with 94% by FDG PET/CT. For N staging, 77% of the patients were correctly staged by FLT and FDG, with 16% of the patients understaged (false-negative) by FLT and 6% by FDG. However, FLT PET/CT had higher specificity (98%) than FDG PET/CT (84%) for the regional lymph node ($p<0.01$). Only 6% of patients were overstaged (false-positive) by FLT PET/CT, while 16% were overstaged by FDG PET/ CT for N staging. Because ^{18}F-FDG is not a tumour-specific tracer, despite high sensitivity, false-positive findings can occur with FDG PET/CT, especially in inflammatory lesions. Accumulation of ^{18}F-FDG in inflammatory cells such as macrophages, fibroblasts, and in some benign tumours can also result in increased FDG uptake because these cells require glucose as their substrate for energy production [2, 3]. Many other factors have been reported to influence ^{18}F-FDG uptake, such as the upregulation of glucose transporter 1 receptors [15].

^{18}F-FLT is a stable tumour cell proliferation imaging agent. It is trapped within the cytosol after being monophosphorylated and enters the exogenous DNA pathway as a specific substrate by the action of thymidine kinase 1 (TK1), a principle enzyme in the salvage pathway of DNA synthesis. Therefore, its accumulation is tightly linked to TK1 enzyme activity [16, 17]. FLT uptake is also dependent on the activity of hexokinase, the ATP level, transportation across cell membranes, and a phosphorylation pathway other than TK1 [18–21]. Many studies have demonstrated increased FLT uptake in tumour tissues [13, 22]. Our study showed that its high specificity and low false-positive rates were an advantage in the diagnosis and staging of NSCLC. However, FLT is not entirely specific for malignant tumours either. In the present study, 6% of patients were overstaged (false-positive) by FLT PET/CT. The mechanism by which FLT produces false-positive results is poorly understood. Pathological examination showed that the lymph nodes false-positive with FLT had reactive hyperplasia and inflammation. A recent study has shown FLT uptake in macrophages of benign nodes and B-lymphocytes in the germinal centres of lymph nodes in patients with head and neck cancer [23]. Some studies have also shown that the FLT uptake could increase in response to active DNA synthesis in any tissue, including growing

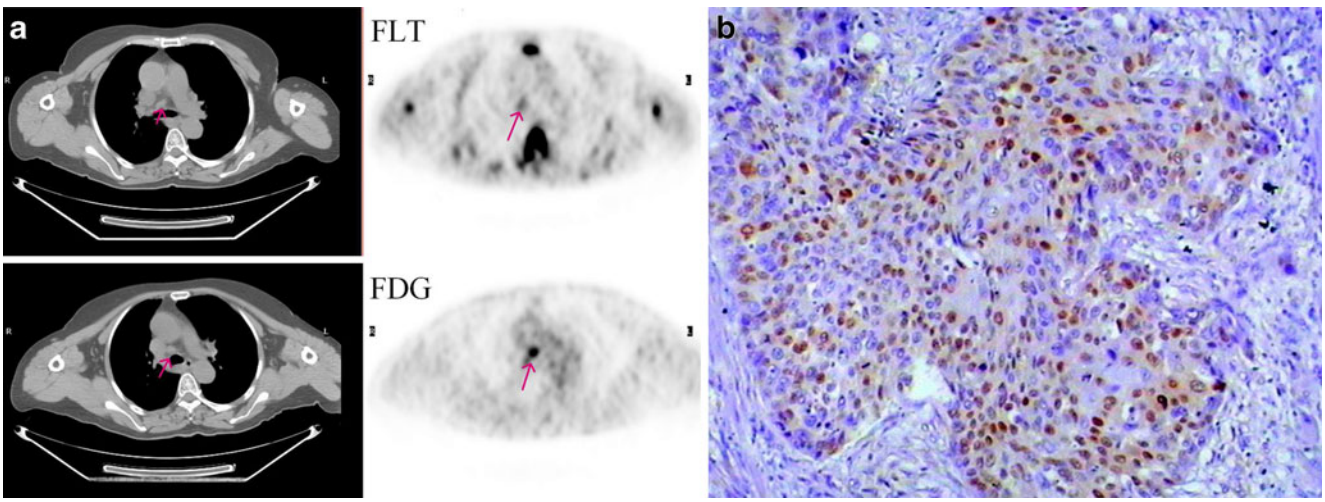

Fig. 1 A 60-year-old woman (patient 22) with adenocarcinoma of the right lower lung lobe: ^{18}F-FLT PET/CT and ^{18}F-FDG PET/CT imaging, cyclin D1 staining. **a** Unenhanced CT and FDG PET images show the pretracheal lymph node (*red arrow*) with FDG uptake (SUVmax 5.6) that was interpreted as true-positive. Unenhanced CT and FLT PET images show the pretracheal lymph node (*red arrow*) with FLT uptake (SUVmax 1.8) that was interpreted as true-positive. **b** Cyclin D1 staining (original magnification ×100)

Table 3 Results of FLT and FDG PET/CT for N staging in the 31 NSCLC patients

PET/CT	Pathological N stage			
	N0 (*n*=13)	N1 (*n*=12)	N2 (*n*=6)	Total (*n*=31)
FLT				
Correctly staged	92% (12/13)	67%(8/12)	67% (4/6)	77% (24/31)
Overstaged (false-positive)	8% (1/13)	8% (1/12)	–	6% (2/31)
Understaged (false-negative)	–	25% (3/12)	33% (2/6)	16% (5/31)
FDG				
Correctly staged	77% (10/13)	75% (9/12)	83% (5/6)	77% (24/31)
Overstaged (false-positive)	23% (3/13)	17% (2/12)	–	16% (5/31)
Understaged (false-negative)	–	8% (1/12)	17% (1/6)	6% (2/31)

microbes [14]. Because of its low sensitivity, high false-negative value, and its nontumour uptake, ^{18}F-FLT was clearly limited for the diagnosis and staging of NSCLC in place of ^{18}F-FDG, but could most probably be used with advantage as an additional tracer to ^{18}F-FDG [13, 22].

Correlation between FLT uptake and cyclin D1 expression in NSCLC

The study found a significant correlation between tumour FLT uptake and cell proliferation indicated by cyclin D1 immunohistochemical staining. Cyclin D1 is the key cell cycle regulatory protein. In proliferating cells, the cyclin D1 complex enters the nucleus and promotes progression from G_1 to S phase, and is then exported from the nucleus and is degraded [24, 25]. Impaired export and degradation can lead to nuclear accumulation of cyclin D1. Nuclear accumulation of cyclin D1 in human bronchial epithelium in situ may facilitate the development of invasive cancer [26, 27]. Positive cyclin D1 immunohistochemical staining has also been found to be a predictor of a poor prognosis in NSCLC, and its expression in tumour cells correlates with their proliferative activity [8, 9]. Therefore, exploring the correlation between the cell cycle by cyclin D1 staining and proliferation imaging by FLT PET may be helpful to further elucidate the mechanism and significance of FLT PET imaging.

Some studies have shown that the expression levels of Ki-67 in resected tissues of NSCLC have prognostic value.

Table 4 Relationship between the mean maximum SUV values of ^{18}F-FLT and ^{18}F-FDG and the clinical and pathological characteristics in the 31 NSCLC patients

Characteristic	No. of patients	SUVmax	
		FLT	FDG
Pathological subtype			
Adenocarcinoma	13	3.8±2.8	8.4±6.0
Squamous carcinoma	11	5.7±4.2	8.1±4.7
Adenosquamous carcinoma	3	3.5±1.1	6.1±0.9
Bronchoalveolar carcinoma	2	1.6±0.4	2.8±0
Large cell neuroendocrine cancer	2	2.8±2.8	7.5±1.1
F		1.07	0.64
p		0.39	0.64
Differentiation			
Well	10	4.1±4.0	5.8±3.9
Moderate	13	3.5±2.8	8.7±6.5
Poor	8	5.5±3.0	8.1±1.6
F		0.85	1.1
p		0.43	0.34
Pathological stage			
I	8	1.7±1.6	4.2±2.3
II	14	3.6±1.9	8.9±6.1
III	9	7.4±3.7	8.9±3.1
F		12.2	3.1
p		0.0002	0.06

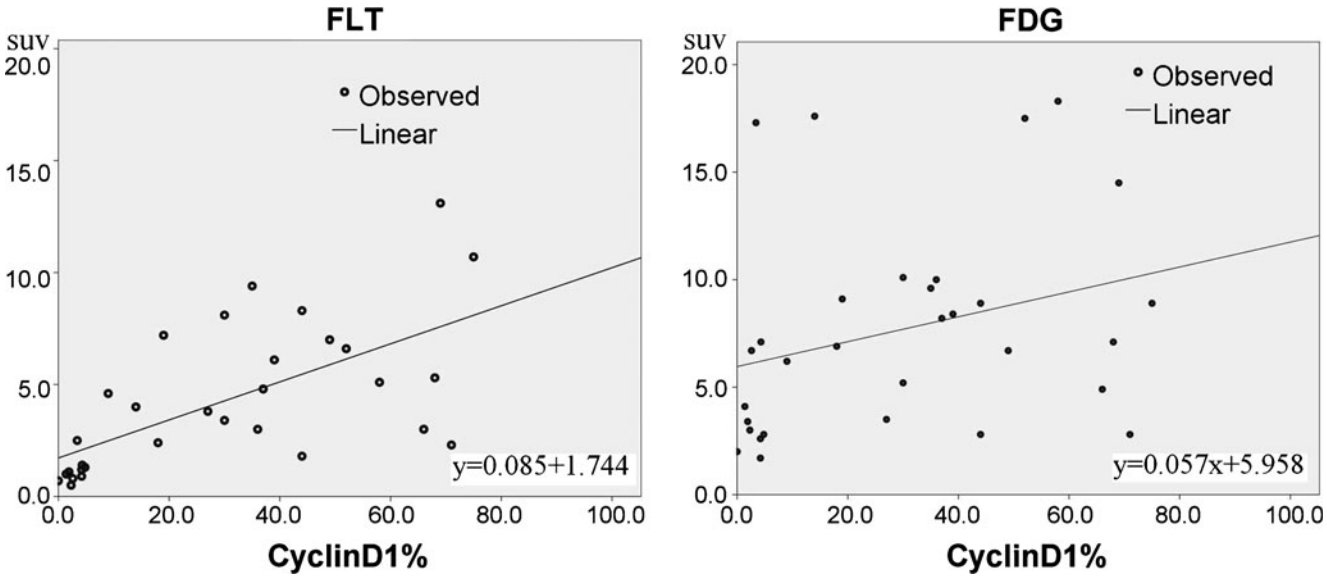

Fig. 2 Correlation between cyclin D1 labelling index and SUV values of FLT and FDG (r=0.644 and 0.293; p=0.0001 and 0.110, respectively)

This approach may have promise in identifying low- and high-grade disease in the initial stages of lung cancer [28]. However, it is not known to what extent the correlation between FLT uptake and cell proliferation is maintained during antitumour therapy. There have been many studies of therapy targeting the tumour cell proliferation cycle. Experiments with antisense cyclin D1 have demonstrated that the active cyclin D1/CDK(cyclin-dependent kinases, CDK) complex is an interesting drug target. The expression of antisense cyclin D1 resulted in decreased proliferation of human oesophageal cancer cells in vitro and in vivo [29]. Small-molecule kinase inhibitors could selectively target the cyclin D1/CDK4 complex to the treatment of lung cancer [30]. Leyton et al. [31] reported that FLT PET could image the changes in cell proliferation following inhibition of mitogenic extracellular kinase 1/2 (MEK1/2) in vivo by the MEK1/2 inhibitor PD0325901. In SKMEL-28 human melanoma cells, the drug rapidly decreased phosphorylated extracellular signal-regulated kinase 1/2, cyclin D1, and thymidine kinase-1 protein levels. Therefore, the significant correlation between FLT uptake and cyclin D1 expression suggests that further studies are needed to evaluate the use of FLT PET/CT for monitoring treatments with cytostatic anticancer drugs.

However, there were some patients in the study with exceptional clinical data, such as patients 16 and 18 who had low FLT SUVmax values (1.8 and 2.3, respectively) and high expression of cyclin D1 (44% and 71%, respectively; Table 1). These exceptional clinical data may have been related to tumour-specific differences in utilization of the thymidine salvage pathway. TK1 is a principle enzyme in the salvage pathway of DNA synthesis. It increases beginning at the G_1/S transition, continues at a high level throughout the S, G_2, and M phases, and then declines rapidly as it is destroyed at the onset of the G_0 or G_1 phase [32]. Loss of cell cycle-specific regulation of TK1 may influence the correlation between FLT uptake and the expression of cyclin D1 [17]. In addition, partial volume effects occur if the lesion size is smaller than three times the spatial resolution of the PET scanner [33, 34]. The lesion in some patients was relatively small, and in these patients calculation of SUVs was to a greater extent confounded by partial volume effects, which could cause an underestimation of the true FLT uptake. To overcome these effects, several correction strategies can be used [35]. For most of them the lesion size needs to be defined and can be measured with high resolution and used to correct the PET data [36, 37]. On the other hand, although the ROI corresponds to the most metabolically active region of the tumour and correlates linearly with tumour proliferation rate, the tumour ROI with the highest SUV (SUVmax) is thought to represent the malignant grade of the tumour overall [38], the use of the SUVmax is the simplest method, with low interobserver variability. The disadvantage of SUVmax is its sensitivity to statistical noise, leading to high fluctuations in the uptake value. To reduce statistical fluctuations, the mean SUV within a defined ROI centred around the voxel with the SUVmax was introduced [28].

In the present study, we used SUVmax for the semiquantitative analysis of FLT and FDG uptake with the advantage of simplicity and low interobserver variability. However, SUVmax is sensitive to statistical noise, leading to high fluctuations in the uptake value. To minimize this effect, we used a fixed number of iterations for the OSEM algorithm (28 subsets, two iterations) [39]. An alternative is the fixed size 2-D average SUV approach as suggested by

Weber et al., which uses a 2-D ROI with a diameter of 1.5 cm around the hottest voxel (i.e. the SUVmax). However, due to the small tumour sizes (<1.5 cm) in the present study, this approach was not utilized. The study was limited by the small number of patients, and the patients admitted to our specialized cancer hospital have already been diagnosed with, or highly suspected of having, lung cancer in other general Hospitals. The pathological examination therefore revealed malignant disease in a high proportion of the enrolled patients, which could have increased the specificity.

Conclusion

This study showed that ^{18}F-FLT PET/CT resulted in more understaged but fewer overstaged patients than ^{18}F-FDG PET/CT for N staging in NSCLC and showed better specificity, accuracy and positive predictive value for the regional lymph nodes than ^{18}F-FDG PET/CT. Tumour FLT uptake was correlated with tumour cell proliferation as indicated by cyclin D1 expression and this suggests the need for further studies to evaluate the use of FLT PET/CT for the assessment of response to anticancer drugs.

Acknowledgments This work was supported by the Research Fund of Shandong Provincial Health Bureau of China (grant 2009HZ088), and by the Research Fund of Shandong Cancer Hospital and Institute (no. 2009-11).

Conflicts of interest None.

References

1. Yamamoto Y, Nishiyama Y, Monden T, et al. Correlation of FDG-PET findings with histopathology in the assessment of response to induction chemoradiotherapy in non-small cell lung cancer. Eur J Nucl Med Mol Imaging 2006;33:140–7.
2. Shim SS, Lee KS, Kim BT, et al. Non-small cell lung cancer: prospective comparison of integrated FDG PET/CT and CT alone for preoperative staging. Radiology 2005;236:1011–9.
3. Yang W, Fu Z, Yu J, et al. Value of PET/CT versus enhanced CT for locoregional lymph nodes in non-small cell lung cancer. Lung Cancer 2008;61:35–43.
4. Mier W, Haberkorn U, Eisenhut M. [18F]FLT: portrait of a proliferation marker. Eur J Nucl Med 2002;29:165–9.
5. Martin B, Paesmans M, Mascaux C, et al. Ki-67 expression and patients survival in lung cancer: systematic review of the literature with meta-analysis. Br J Cancer 2004;91:2018–25.
6. Au NH, Cheang M, Huntsman DG, et al. Evaluation of immunohistochemical markers in non-small cell lung cancer by unsupervised hierarchical clustering analysis: a tissue microarray study of 284 cases and 18 markers. J Pathol 2004;204:101–9.
7. Saitoh G, Sugio K, Ishida T, et al. Prognostic significance of p21waf1, cyclin D1 and retinoblastoma expression detected by immunohistochemistry in non-small cell lung cancer. Oncol Rep 2001;8:737–43.
8. Jin M, Inoue S, Umemura T, et al. Cyclin D1, p16 and retinoblastoma gene product expression as a predictor for prognosis in non-small cell lung cancer at stages I and II. Lung Cancer 2001;34:207–18.
9. Oshita F, Ito H, Ikehara M, et al. Prognostic impact of survivin, cyclin D1, integrin beta1, and VEGF in patients with small adenocarcinoma of stage I lung cancer. Am J Clin Oncol 2004;27:425–8.
10. Buck AK, Schirrmeister H, Hetzel M, et al. 3-deoxy-3-[(18)F] fluorothymidine-positron emission tomography for noninvasive assessment of proliferation in pulmonary nodules. Cancer Res 2002;62:3331–4.
11. Vesselle H, Grierson J, Muzi M, et al. In vivo validation of 3′ deoxy-3′-[(18)F]fluorothymidine ([(18)F]FLT) as a proliferation imaging tracer in humans: correlation of [(18)F]FLT uptake by positron emission tomography with Ki-67 immunohistochemistry and flow cytometry in human lung tumors. Clin Cancer Res 2002;8:3315–23.
12. Goldstraw P, Crowley J, Chansky K, et al. The IASLC Lung Cancer Staging Project: proposals for the revision of the TNM stage groupings in the forthcoming (seventh) edition of the TNM Classification of malignant tumours. J Thorac Oncol 2007;2:706–14.
13. Yamamoto Y, Nishiyama Y, Kimura N, et al. Comparison of (18) F-FLT PET and (18)F-FDG PET for preoperative staging in non-small cell lung cancer. Eur J Nucl Med Mol Imaging 2008;35:236–45.
14. Tian J, Yang X, Yu L, Chen P, Xin J, Ma L, et al. A multicenter clinical trial on the diagnostic value of dual-tracer PET/CT in pulmonary lesions using 3′-deoxy-3′-18F-fluorothymidine and 18F-FDG. J Nucl Med 2008;49:186–94.
15. Marom EM, Aloia TA, Moore MB, et al. Correlation of FDG-PET imaging with Glut-1 and Glut-3 expression in early-stage non-small cell lung cancer. Lung Cancer 2001;33:99–107.
16. Rasey JS, Grierson JR, Wiens LW, et al. Validation of FLT uptake as a measure of thymidine kinase-1 activity in A549 carcinoma cells. J Nucl Med 2002;43:1210–7.
17. Schwartz JL, Tamura Y, Jordan R, et al. Monitoring tumor cell proliferation by targeting DNA synthetic processes with thymidine and thymidine analogs. J Nucl Med 2003;44:2027–32.
18. Dimitrakopoulou-Strauss A, Strauss LG. The role of 18F-FLT in cancer imaging: does it really reflect proliferation? Eur J Nucl Med Mol Imaging 2008;35:523–6.
19. Leyton J, Latigo JR, Perumal M, Dhaliwal H, He Q, Aboagye EO. Early detection of tumor response to chemotherapy by 3′-deoxy-3′-[18F]fluorothymidine positron emission tomography: the effect of cisplatin on a fibrosarcoma tumor model in vivo. Cancer Res 2005;65:4202–10.
20. Reske SN, Deisenhofer S. Is 3′-deoxy-3′-(18)F-fluorothymidine a better marker for tumour response than (18)F-fluorodeoxyglucose? Eur J Nucl Med Mol Imaging 2006;33 Suppl 1:38–43.
21. Wieder HA, Geinitz H, Rosenberg R, et al. PET imaging with [18F]3′-deoxy-3′-fluorothymidine for prediction of response to neoadjuvant treatment in patients with rectal cancer. Eur J Nucl Med Mol Imaging 2007;34:878–83.
22. Yap CS, Czernin J, Fishbein MC, et al. Evaluation of thoracic tumors with 18F-fluorothymidine and 18F-fluorodeoxyglucose-positron emission tomography. Chest 2006;129:393–401.
23. Troost EG, Vogel WV, Merkx MA, et al. 18F-FLT PET does not discriminate between reactive and metastatic lymph nodes in primary head and neck cancer patients. J Nucl Med 2007;48:726–35.
24. Kato JY, Matsuoka M, Strom DK, et al. Regulation of cyclin D-dependent kinase 4 (cdk4) by cdk4-activating kinase. Mol Cell Biol 1994;4:2713–21.
25. Gautschi O, Ratschiller D, Gugger M, et al. Cyclin D1 in non-small cell lung cancer: a key driver of malignant transformation. Lung Cancer 2007;55:1–14.

26. Ratschiller D, Heighway J, Gugger M, et al. Cyclin D1 overexpression in bronchial epithelia of patients with lung cancer is associated with smoking and predicts survival. J Clin Oncol 2003;21:2085–93.
27. Benzeno S, Lu F, Guo M, et al. Identification of mutations that disrupt phosphorylation-dependent nuclear export of cyclin D1. Oncogene 2006;25:6291–303.
28. Soomro IN, Holmes J, Whimster WF. Predicting prognosis in lung cancer: use of proliferation marker, Ki67 monoclonal antibody. J Pak Med Assoc 1998;48:66–9.
29. Zhou P, Jiang W, Zhang YJ, et al. Antisense to cyclin D1 inhibits growth and reverses the transformed phenotype of human esophageal cancer cells. Oncogene 1995;11:571–80.
30. Fry DW, Harvey PJ, Keller PR, et al. Specific inhibition of cyclin-dependent kinase 4/6 by PD-0332991 and associated antitumor activity in human tumor xenografts. Mol Cancer Ther 2004;3:1427–38.
31. Leyton J, Smith G, Lees M, et al. Noninvasive imaging of cell proliferation following mitogenic extracellular kinase inhibition by PD0325901. Mol Cancer Ther 2008;7:3112–21.
32. Arnér ES, Eriksson S. Mammalian deoxyribonucleoside kinases. Pharmacol Ther 1995;67:155–86.
33. Hoffman EJ, Huang SC, Phelps ME. Quantitation in positron emission computed tomography: 1. Effect of object size. J Comput Assist Tomogr 1979;3:299–308.
34. Soret M, Bacharach SL, Buvat I. Partial-volume effect in PET tumor imaging. J Nucl Med 2007;48:932–45.
35. Rousset O, Rahmim A, Alavi A, et al. Partial volume correction strategies in PET. PET Clinics 2007;2:235–49.
36. Pottgen C, Levegrun S, Theegarten D, et al. Value of 18F-fluoro-2-deoxy-D-glucose-positron emission tomography/computed tomography in non-small-cell lung cancer for prediction of pathologic response and times to relapse after neoadjuvant chemoradiotherapy. Clin Cancer Res 2006;12:97–106.
37. Hickeson M, Yun M, Matthies A, et al. Use of a corrected standardized uptake value based on the lesion size on CT permits accurate characterization of lung nodules on FDG-PET. Eur J Nucl Med Mol Imaging 2002;29:1639–47.
38. Vesselle H, Schmidt RA, Pugsley JM, et al. Lung cancer proliferation correlates with F-18 fluorodeoxyglucose uptake by positron emission tomography. Clin Cancer Res 2000;6:3837–44.
39. Jaskowiak CJ, Bianco JA, Perlman SB, Fine JP. Influence of reconstruction iterations on 18F-FDG PET/CT standardized uptake values. J Nucl Med 2005;46:424–8.